Appendix A

Prototype RICH Test Results

Key elements of the proposed RICH detector have been subjected to in-beam testing in RHIC RD44 using secondary beams at the AGS, and some pertinent results are reported here. Note that the multi-anode PMT used in these tests was the first version of its kind to meet the specifications of the Hamamatsu Corporation, upon which the expected performance criteria outlined in Sect. 7.4 are based.

A.1 The Multi-anode PMT

The R-4549-01 is a 20-stage 100-anode PMT based on a fine-mesh dynode structure, providing a current gain of 3×10^6 at a high voltage of HV = 2000 volts. The 10×10 cm^2 photocathode is bialkali: the segmented anode is a matrix array ($10\times10 = 100$) of 9.5×9.5 mm^2 units with lemo outputs. With current gains of 10^6 - 2×10^7 (HV = 1800-2500 volts) the outputs will easily drive cable connections to appropriate ADC's. The high voltage is supplied by a single high-voltage cable: a built-in R/C dropping chain fixes the relative dynode voltages. A single output from the last dynode, representing essentially the "sum" of all anode currents, is available as a convenient gate.

The entrance window is of boro-silicate glass with the typical cutoff for wavelengths $\lambda < 300$ nm ($E > 4.1$ eV). The quantum efficiency response function is approximately Gaussian, with a peak sensitivity of 18%, centered at $E = 3.4$ eV and with FWHM = 1.8 eV. (The tails, however, fall off twice as fast as a true Gaussian.) As given in the above section on the RICH counter, the energy integral for the PMT efficiency is $\int \epsilon(E)dE = 0.33$ eV.

A.2 PMT Single-photon Response

Since the Čerenkov ring-image is composed of multiple hits of single photons, we were prompted to study the single-hit response. For this purpose, the R-4549 PMT was first mounted in a light-tight box. A collimated photon source, using a blue LED, was positioned a few cm away from the photocathode; the collimator opening was such as to illuminate only a single pixel at a time. The LED was pulsed by a driver whose intensity could be tuned low enough so that the collimator output was either 0 or 1 photon. (This tuning requirement was checked independently using a special RCA PMT with excellent single-photon resolution.) The data acquisition was triggered by the same signal which triggered the LED. The position dependence of the response is shown in Fig. A.1. The relative signal in each of three adjacent pixels is plotted for a run in which the position of the LED relative to the phototube was stepped in the y-direction. The FWHM of the response for an individual pixel is 10 mm with little cross-talk between neighboring pixels, as expected. In general, the pulse heights in neighboring pixels average only about 10% of that in the hit pixel.

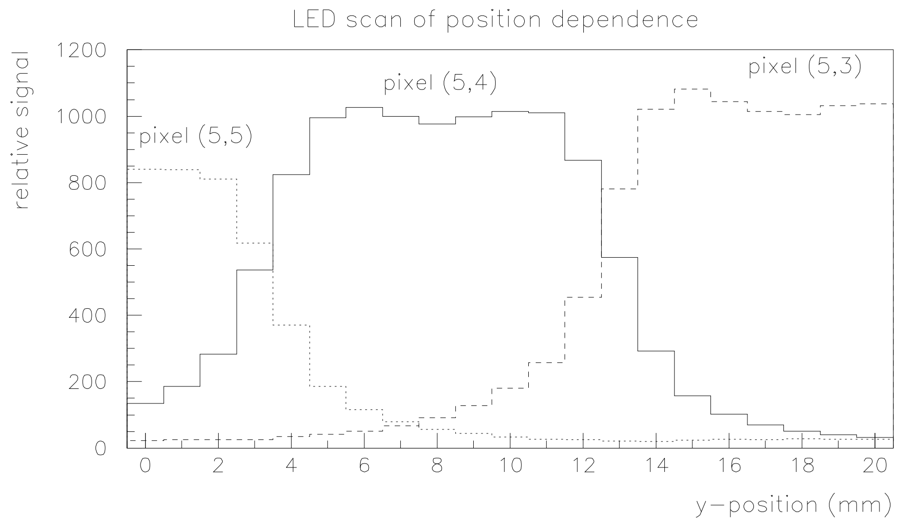

Figure A.1: Position dependence of the PMT pulse height in three adjacent pixels, measured as the position of an LED is stepped with respect to the phototube.

A.3 The Test Box

The test box is shown schematically in Fig. A.2. It was constructed from 1.9 cm thick aluminum plate, vacuum-welded at the box edges, with a removable top attached by 50

1/4-20 screws and sealed by a rubber gasket. The inner dimensions are $127\times64\times46$ cm^3. The particle beam enters via a 15 cm diameter mylar window of thickness 0.025 mm (shown on the left in the figure) and exits through an identical window at the output port.

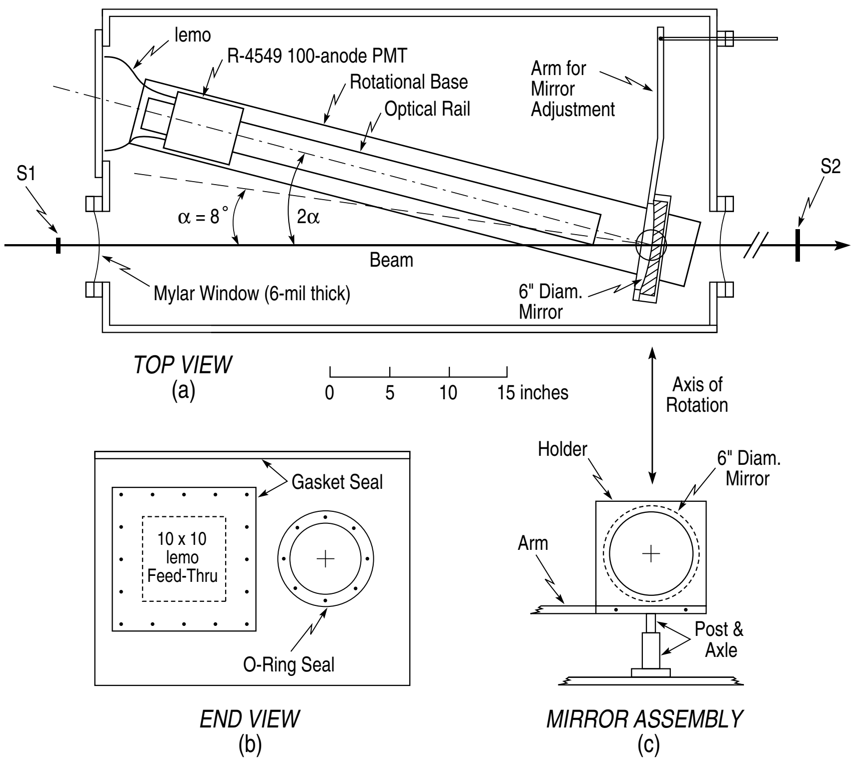

Figure A.2: Schematic view of the RICH test box. See text for details.

A 15 cm diameter mirror of multi-layer dielectric-coated aluminum with a focal length $f = 91$ cm is situated at a distance of $L = 114$ cm from the beam entrance, and is rotated by an angle $\alpha = 8°$ relative to the beam direction, producing a ring image focussed at $2\alpha = 16°$. The mirror was mounted in a frame attached to an axle which could be rotated about a vertical axis perpendicular to the beam direction. The mirror angle was controlled by a 0.6 cm steel rod which moved a 47 cm arm rigidly fixed to the mirror frame, so as to allow a mirror rotation over the range $-12° < \alpha < +12°$.

One hundred six Lemo signal cables are fed into the box using ordinary Lemo feed-throughs epoxyed into place to maintain a vacuum seal.

The device was aligned in the secondary test beam at the AGS, with the trigger defined by a 2×2 cm^2 scintillator, S1, just before the entrance window of the test vessel, and a larger scintillator paddle, S2, downstream of the exit window. Two drift chambers, one in front of and one behind the test box, provided tracking for determining the particle trajectory, and hence measured the expected position of the center of the RICH ring to better than 1 mm in both the x and y directions.

A.4 Gas Handling System

The gas-handling system used in filling the RICH chamber with fluorocarbons is shown in Fig. A.3. The procedure adopted utilizes the fact that the radiator gases Freon-12 (122) and C_4F_{10} (238) have molecular weights (given in parentheses) much heavier than air (29) or argon (39). For example, consider the case where the RICH chamber has been initially filled with argon. The C_4F_{10} is set to flow slowly into the bottom of the vessel, while the output mixture (Ar + C_4F_{10}) is sent through a cooled recovery tank where the C_4F_{10} is liqified while the argon passes out the exhaust. The differing molecular weights (factor of 6) result in a density gradient in the RICH vessel, such that if the flow is slow enough (non-turbulent) the volume slowly becomes enriched in C_4F_{10}. The procedure can be continued until the supply in tank A is exhausted. In our case we manually switched the two tanks A and B and repeated the cycle using the C_4F_{10} previously recovered in B. Three such cycles yielded a gas mix of approximately 90% purity in C_4F_{10}.

In order to recover the C_4F_{10} at the conclusion of the experiment, a pump was used to reverse the flow direction – as indicated by the dashed lines in Fig. A.3. As the C_4F_{10} is recovered into B, the observed pressure drop in the chamber is compensated by adding argon to maintain a pressure differential of < 0.15 atm.

In principle, one can install a remote-controlled switching system to actuate the controlling valves, so as to alternate the designated funtion of the supply and recovery tanks. This would allow an extended period of automatic cycling, leading to a nearly 100% purity of C_4F_{10}, or by reversing the cycle, a complete recovery of the fluorocarbon.

A.5 In-Beam Testing

Figure A.4 presents results measured with the beam tuned for negative 12 GeV/c particles — predominantly pions — and a gas mixture in the test box of Freon-12 and N_2. Panel (a) shows the pulse height for each phototube pixel, summed over approximately 1100 events. The drawn ring is the best fit of the data to a circle. Figure A.4b is a histogram of the ADC pulse height in pixel (3,8), which lies directly on the ring. The corresponding histogram from neighboring pixel (3,9), which is not on the ring, is shown in Fig. A.4c; clearly the cross-talk between adjacent pixels is small, although not completely negligible.

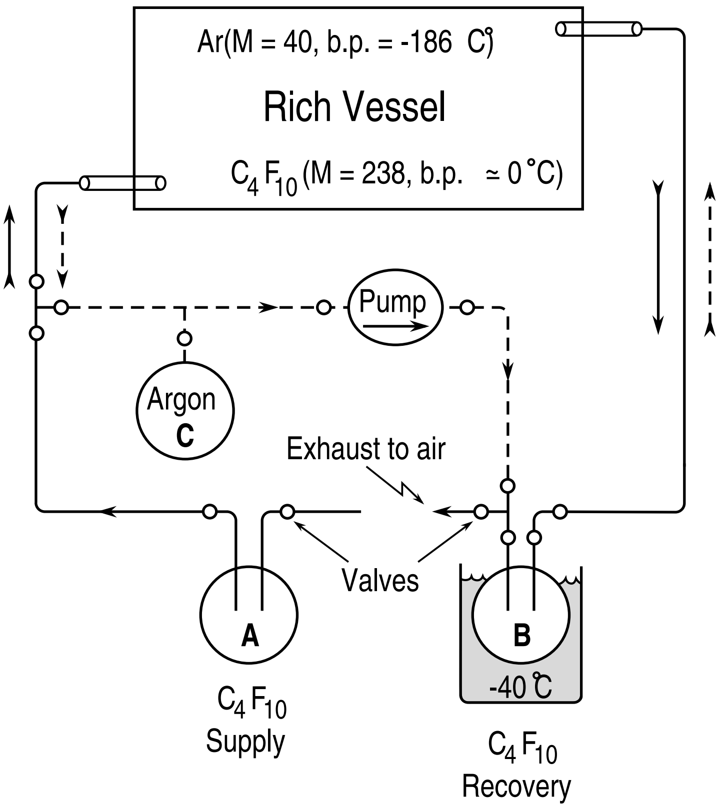

Figure A.3: Schematic flow-diagram for gas-handling system. Solid lines are for initial filling with the fluorocarbon; dashed lines (note reversed direction) are for final recovery of the fluorocarbon gas. With this system, the pressure in the RICH vessel can be kept within $< 10\%$ of atmospheric over both the filling and recovery operations.

The ability of the counter to identify individual particles is demonstrated in Fig. A.5. Panels a, b and c show individual events from a run where the beam momentum was tuned to 3 GeV/c and the box contained a C_4F_{10}-Ar mixture. The drawn rings show the best fits to circles constrained by the positions of the ring center (shown as the small star symbols) given independently by the drift chamber tracking. The ring radius from all events in the run is histogrammed in Fig. A.5d where three distinct peaks, identified with π^-, μ^- and e^-, are clearly observed. The peaks are well described as gaussian in shape; for the rings which are fully saturated in radius (electrons) the resolution of the radius determination is $\sigma_r/r = 2.3\%$.

A momentum scan was performed with a C_4F_{10}-Ar mixture in the vessel during a period in which the ratio of the gases did not change. The ring radius is plotted versus momentum in Fig. A.6, which shows saturated light production from electrons, as well as the excitation curves for muons, pions and kaons. The saturated radius for

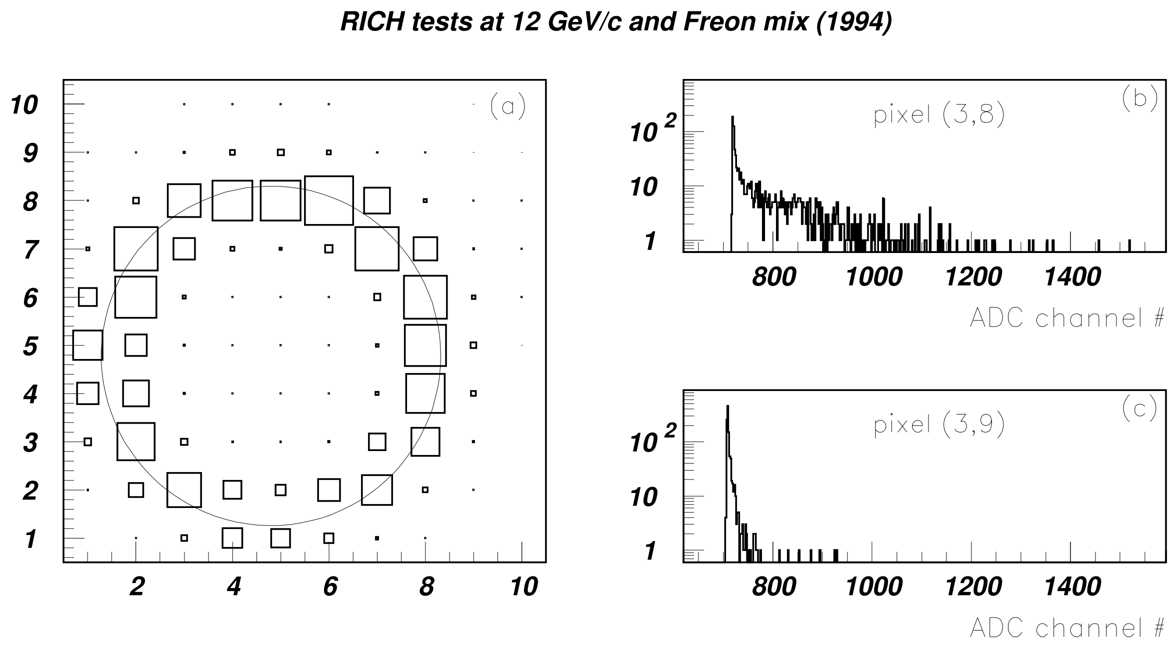

Figure A.4: Results from the prototype RICH counter with test beam at 12 GeV/c and a Freon gas mixture. Panel a shows a ring image from approximately 1100 events and panels b and c show the ADC pulse height spectra from two individual pixels. See text for details.

electrons implies an index of refraction n=1.00113, shown as the horizontal line through the electron points. (This includes a 3% correction to the radius to account for the fact that the position of phototube was for practical reasons slightly out of the focal plane.) The excitation curves predicted by this index of refraction are shown as the solid curves; the shaded regions represent a $\pm$5% systematic uncertainty in the absolute momentum scale. The measured values of the radius all lie within the shaded regions. From n=1.00113 it is inferred that the fraction of C_4F_{10} in the vessel was approximately 75%. Later runs following further filling of the vessel achieved approximately 90% C_4F_{10}.

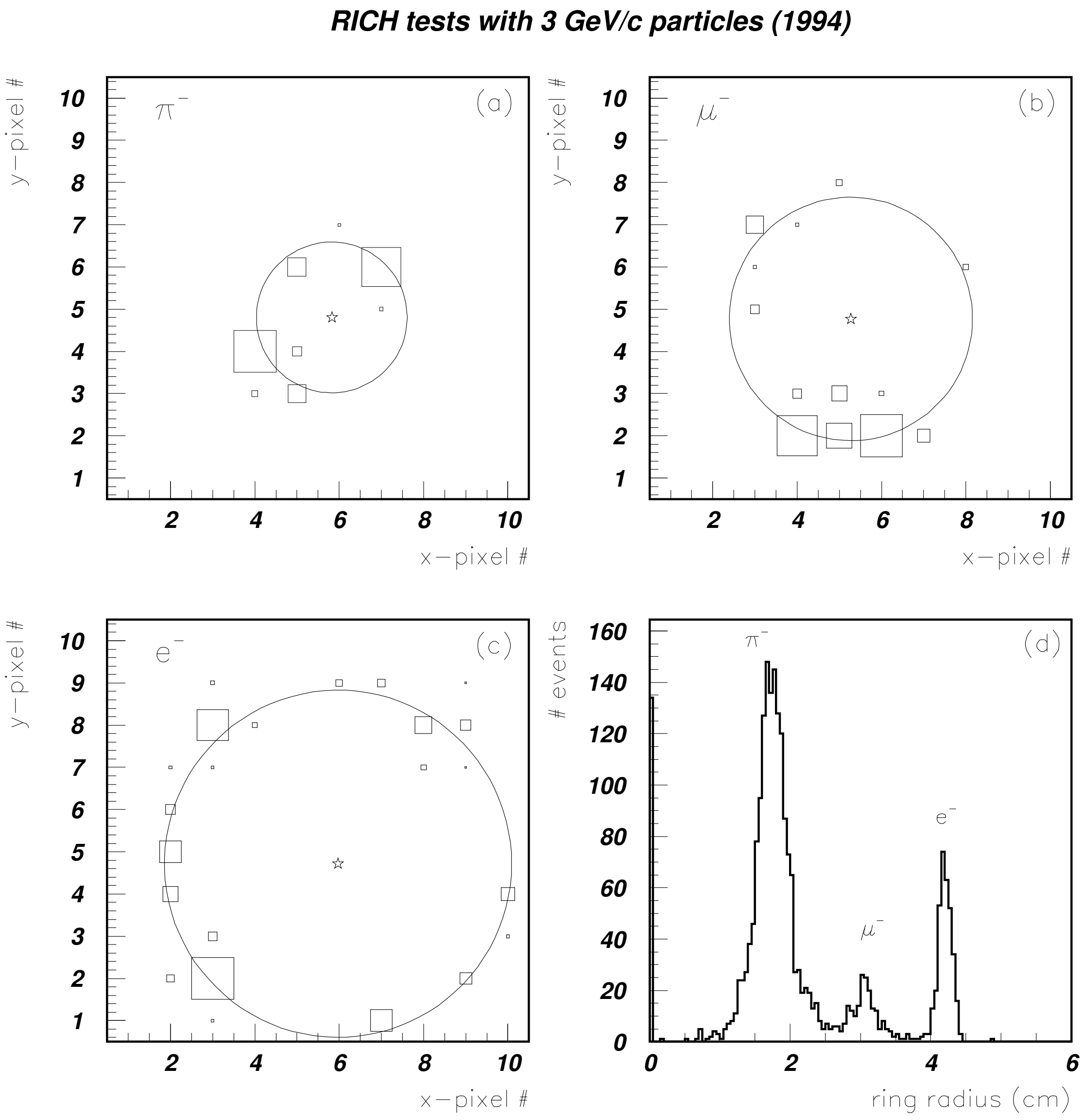

Figure A.5: Results from the prototype RICH counter with test beam at 3 GeV/c and a C_4F_{10}-Ar gas mixture. Panels a, b and c show individual events with fitted rings; the ring centers are shown as stars and come from independent drift chamber tracking. Panel d is a histogram of the fitted ring radius from the entire run, showing peaks identified as π^-, μ^- and e^-.

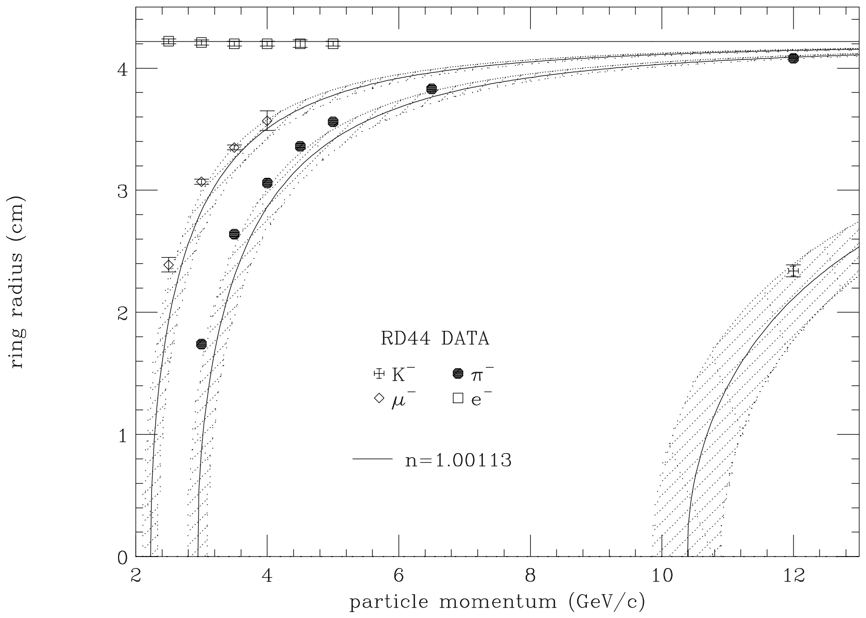

Figure A.6: The mean radius from event-by-event fits to rings in the prototype RICH counter filled with a C_4F_{10}-Ar gas mixture, for different particle species. The solid curves show the expected radii for an index of refraction of $n = 1.00113$; the shaded regions represent a 5% systematic uncertainty in the absolute momentum scale.